11158 *Inorg. Chem.* **2010**, *49*, 11158–11163
DOI: 10.1021/ic101786r

Inorganic Chemistry
Article

Systematic and In Situ Energy Dispersive X-ray Diffraction Investigations on the Formation of Lanthanide Phosphonatobutanesulfonates: $Ln(O_3P\text{-}C_4H_8\text{-}SO_3)(H_2O)$ (Ln = La−Gd)

Mark Feyand,[†] Christian Näther,[†] André Rothkirch,[‡] and Norbert Stock*[,†]

[†]*Institut für Anorganische Chemie, Christian-Albrechts-Universität, Max-Eyth Strasse 2, D 24118 Kiel, Germany, and* [‡]*HASYLAB, DESY Hamburg, Notkestrasse 85, 22607 Hamburg, Germany*

Received September 1, 2010

Using the flexible linker $H_2O_3P\text{-}C_4H_8\text{-}SO_3H$ (H_3L) and rare earth ions Ln^{3+} (Ln = La, Ce, Pr, Nd, Sm, Eu, Gd) we were able to synthesize the new isostructural inorganic organic hybrid compounds $Ln(O_3P\text{-}C_4H_8\text{-}SO_3)(H_2O)$. High-throughput experiments were employed to study the influence of the molar ratios Ln:H_3L and pH on the product formation. The crystal structure of the compounds $Sm(O_3P\text{-}C_4H_8\text{-}SO_3)(H_2O)$ (**1**) and $Pr(O_3P\text{-}C_4H_8\text{-}SO_3)(H_2O)$ (**2**) were determined by single crystal diffraction. The structures are built up from chains of edge-sharing LnO_8-polyhedra that are connected by the phosphonate and sulfonate groups into layers. These layers are linked by the $-(CH_2)_4-$ group to form a three-dimensional framework. The synthesis of compound **1** was scaled up in a conventional oven as well as in a microwave reactor system. A modification of a microwave reactor system allowed its integration into the beamline F3 at HASYLAB, DESY, Hamburg. The crystallization was investigated in situ by means of energy dispersive X-ray diffraction using conventional as well as microwave heating methods applying temperatures varying from 110 to 150 °C. The formation of $Sm(O_3P\text{-}C_4H_8\text{-}SO_3)(H_2O)$ takes place in two steps. In the first step a crystalline intermediate was observed, which transforms completely into compound **1.** The method by Sharp and Hancock was used to determine the rate constants, reaction exponents, and the Arrhenius activation energy for both reaction steps. Comparing both heating methods, microwave heating leads to fully crystallized reaction product after shorter reaction times, but neither the temperature nor the heating method has significant influence on the induction time.

Introduction

Inorganic−organic hybrid compounds are currently under intensive investigations because of their potential application in gas storage, catalysis, or charge storage materials.[1,2] Most of these compounds are based on polycarboxylates, -phosphonates, or -sulfonates.[3,4] Different polyfunctionalized organic building units containing two or more functional groups have been used less often. In the field of metal phosphonates these mainly include phosphonocarboxylic acids[5−7] and aminophosphonic acids.[8,9] Very recently phosphonatosulfonic acids have also come into the focus of interest.[10−14]

The majority of known metal phosphonatosulfonates are based on rigid organic building units, that is, *m*- and *p*-sulfophenylphosphonic acid. In combination with co-ligands often M-O-Clusters are obtained.[15−20] Such compounds show a large structural variety ranging from isolated cluster,[15,18,19] one-dimensional chains[18] to three-dimensional frameworks.[16] We are interested in the synthesis of hybrid compounds with flexible phosphonosulfonic acids and have therefore synthesized and

*To whom correspondence should be addressed. Phone: +49-431-880-1675. Fax: +49-431-880-1775. E-mail: stock@ac.uni-kiel.de.

(1) Clearfield, A. *Prog. Inorg. Chem.* **1998**, *47*, 371–510.
(2) Czaja, A. U.; Trukhan, N.; Müller, U. *Chem. Soc. Rev.* **2009**, *38*, 1284.
(3) Shimizu, G. K. H.; Vaidhyanathan, R.; Taylor, J. M. *Chem. Soc. Rev.* **2009**, *38*, 1430.
(4) Rowsell, J. L. C.; Yaghi, O. M. *Microporous Mesoporous Mater.* **2004**, *73*, 3.
(5) Bauer, S.; Marrot, J.; Devic, T.; Férey, G.; Stock, N. *Inorg. Chem.* **2007**, *46*(23), 9998–10002.
(6) Bauer, S.; Bein, T.; Stock, N. *Solid State Sci.* **2008**, *10*(7), 837–846.
(7) Stock, N.; Frey, S. A.; Stucky, G. D.; Cheetham, A. K. *J. Chem. Soc., Dalton Trans.* **2000**, 4292–4296.
(8) Cao, G.; Hong, H. G.; Mallouk, T. E. *Acc. Chem. Res.* **1992**, *25*(9), 420–427.
(9) Casciola, M.; Costantino, U.; Peraio, A.; Rega, T. *Solid State Ionics* **1995**, *77*, 229–233.
(10) Sonnauer, A.; Stock, N. *Eur. J. Inorg. Chem.* **2008**, 5038.
(11) Sonnauer, A.; Feyand, M.; Stock, N. *Cryst. Growth Des.* **2008**, *9*(1), 586–592.
(12) Sonnauer, A.; Näther, C.; Höppe, H. A.; Senker, J.; Stock, N. *Inorg. Chem.* **2007**, *46*(23), 9968–9974.
(13) Sonnauer, A.; Stock, N. *Inorg. Chem.* **2005**, *2007*(44), 5882.
(14) Sonnauer, A.; Stock, N. *J. Solid State. Chem.* **2008**, *181*, 473.
(15) Du, Z.-Y.; Xu, H.-B.; Mao, J.-G. *Inorg. Chem.* **2006**, *45*, 9780.
(16) Du, Z.-Y.; Xu, H.-B.; Mao, J.-G. *Inorg. Chem.* **2006**, *45*, 6424.
(17) Du, Z.-Y.; Xie, Y.-R.; Wen, H. R. *Acta Crystallogr., Sect. E* **2007**, *E63*, M2766.
(18) Du, Z.-Y.; Prosvirin, V. A.; Mao, J.-G. *Inorg. Chem.* **2007**, *46*, 9884.
(19) Du, Z.-Y.; Li, X.-L.; Liu, Q.-Y.; Mao, J.-G. *Cryst. Growth Des.* **2007**, *7*, 1501.
(20) Du, Z.-Y.; Xu, H.-B.; Li, X.-L.; Mao, J.-G. *Eur. J. Inorg. Chem.* **2007**, 4520.

Published on Web 11/08/2010

employed the phosphonosulfonic acids with different chain lengths H_2O_3P-C_2H_4-SO_3H[10,12−14,21] and H_2O_3P-C_4H_8-SO_3H.[11]

These metal phosphonatosulfonates have been synthesized under solvothermal reaction conditions. Small variations in the reaction conditions often lead to new compounds resulting in complex crystallization diagrams. Mostly conventional heating methods have been used, and recently a study employing microwave assisted heating has been described.[21] An acceleration of the product formation compared to conventional heating was observed. The influence of heating by microwave irradiation is discussed controversially in the literature.[22,23] Some authors attribute the differences to thermal as well as non-thermal microwave effects.

To investigate the multiparameter space of such systems, high-throughput (HT) methods have been shown to accelerate the discovery of compounds and the synthesis optimization, as well as the determination of reaction trends.[24−26] Thus, HT studies allow to systematically investigate the influence of different parameters such as the pH of the reaction mixture,[27] the reaction temperature,[28] the molar ratios of reactants,[29] and the nature of solvents.[5,30] Although HT methods allow for effective study of reaction systems, they do not reveal information on the crystallization rate or mechanism.

The crystallization can be studied by energy dispersive X-ray diffraction (EDXRD) measurements.[31−34] White beam synchrotron radiation is widely used to achieve a time resolution below one minute per spectrum. Employing this method, for example, the crystallization of zeolithes,[34] thioantimonates,[32] metal−organic frameworks (MOFs),[33] or the breathing effect of flexible MOFs[35] was investigated. EDXRD measurements allow the monitoring of the crystallization and thus offer the possibility to observe crystalline intermediate phases. These can either be isolated by quenching[33] or are only stable in the reaction mixture.[33,36] Applying the Avrami−Eroféev equation and the method of Sharp and Hancock to the data, kinetic analyses yield the rate constants and information on the possible reaction mechanism.[37] This allows to study the influence of reaction temperatures and concentrations on the crystallization and the mechanism.[36] In case of temperature dependent EDXRD studies, the Arrhenius activation energies can be calculated.[31,32,36,38,39]

In this study we describe a systematic investigation of the rare earth phosphonatosulfonates $Ln(O_3P$-C_4H_8-$SO_3)(H_2O)$ (Ln = La−Gd) by HT methods and the first temperature dependent EDXRD on the formation of metal phosphonates. The influence of heating methods is studied by carrying out reactions under microwave as well as conventional heating which required the implementation of a microwave reactor system at beamline F3, HASYLAB, Hamburg.

Experimental Section

4-Phosphonobutanesulfonicacid H_2O_3P-C_4H_8-SO_3H (H_3L) was synthesized as previously reported in the literature in a two step nucleophile substitution reaction of 1,4-dibromobutane with triethylphosphite and sodium sulfite.[11] All other reagents were of analytical grade (Fluka and Aldrich) and were used without further purification. HT-X-ray powder diffraction (XRPD) measurements were carried out on a Stoe Stadi P HT-diffractometer in transmission geometry with Cu $K_{\alpha 1}$ radiation, equipped with an image plate detector. MIR spectra were recorded on an ATI Matheson Genesis in the spectral range 4000−400 cm^{-1} (2.5−25 μm) using the KBr disk method. For the thermogravimetric analysis under air a NETSCH STA 409 CD analyzer was used with a heating rate of 4 K/min (flow rate: 75 mL/min).

HT Experiments. The system $SmCl_3/H_3L/NaOH$ in water was investigated by using HT methods. All reagents were dispensed as aqueous solutions. The experiments were carried out to investigate the influence of the molar ratios $H_3L/SmCl_3$ and the pH on the product formation. A custom-made HT reactor containing 48 PTFE linears each with a maximum volume of 300 μL was used.[40] Different combinations of molar ratios $SmCl_3/H_3L/NaOH$ varying from 1−4:1−4:0−10 were investigated. The solutions were added to the PTFE inserts, homogenized by stirring, and heated in 15 h to 150 °C, held at that temperature for 48 h, and then cooled down to room temperature in 15 h. The products were filtered off, washed with water, dried in air and characterized by XRPD measurements. Details of the exact amounts employed and the reaction products are given in Supporting Information, Table S1. The pH values of all starting mixtures were measured using pH paper with an error range of ±1.

Scale-up Synthesis. Larger amounts of compound **1** were obtained using the optimized synthesis conditions as derived from the HT study. A 146 μL portion of an aqueous 4 M H_3L solution, 1560 μL of water, 146 μL of an aqueous 2 M $SmCl_3$ solution, and 292 μL of a 4 M NaOH solution were added into a Schott Duran glass culture tubes (Gl-14), mixed by shaking and heated in an oven for 15 h at 150 °C. The white solid was isolated and washed with water yielding an amount of 80.6 mg (72% based on H_3L).

Microwave Synthesis. Exactly the same amounts of base materials were used for the microwave assisted synthesis. The solutions of the base materials were mixed in a microwave tube (Biotage, 0.5−2 mL glass reactor), sealed with a septum, mixed by shaking, and heated in a microwave oven (Biotage Injector) for 4 h at 150 °C. The white solid was isolated by filtration and washed with water yielding an amount of 73.9 mg (66% based on H_3L).

Synthesis of $Ln(O_3P$-C_4H_8-$SO_3)(H_2O)$ (Ln = La−Gd). Isostructural rare earth compounds were obtained applying the optimized synthesis conditions of the Sm compound as derived from the HT study. The HT reactors were used, and 15 μL of a 4 M H_3L solution, 156.0 μL of water, 15 μL of a 2 M LnX_3 (LnX_3 = $La(NO_3)_3$, $Ce(NO_3)_3$, $Pr(NO_3)_3$, $Nd(NO_3)_3$, $Eu(NO_3)_3$, $Gd(CH_3CO_2)_3$), and 15 μL of 4 M NaOH were mixed in the 300 μL PTFE inserts. The mixtures were homogenized by shaking and heated in an oven for

(21) Sonnauer, A.; Stock, N. *J. Solid State Chem.* **2008**, *181*, 3065.
(22) Hoz, A. d. l.; Diaz-Ortiz, A.; Moreno, A. *Chem. Soc. Rev.* **2005**, *34*, 164.
(23) Obermayer, D.; Gutmann, B.; Kappe, C. O. *Angew. Chem., Int. Ed.* **2009**, *48*(44), 8321–8324.
(24) Corma, A.; Diaz-Cabanas, M. J.; Jorda, J. L.; Martinez, C.; Moliner, M. *Nature* **2006**, *443*(7113), 842–845.
(25) Banerjee, R.; Phan, A.; Wang, B.; Knobler, C.; Furukawa, H.; O'Keeffe, M.; Yaghi, O. M. *Science* **2008**, *319*, 939.
(26) Stock, N. *Microporous Mesoporous Mater.* **2009**, *3*, 287.
(27) Stock, N.; Bein, T. *Angew. Chem., Int. Ed.* **2004**, *43*(6), 767–770.
(28) Bauer, S.; Stock, N. *Angew. Chem., Int. Ed.* **2007**, *46*(36), 6857–6860.
(29) Stock, N.; Bein, T. *J. Mater. Chem.* **2005**, *15*, 1384.
(30) Ahnfeldt, T.; Guillou, N.; Gunzelmann, D.; Margiolaki, I.; Loiseau, T.; Férey, G.; Senker, J.; Stock, N. *Angew. Chem., Int. Ed.* **2009**, *48*(28), 5163.
(31) Engelke, L.; Schaefer, M.; Porsch, F.; Bensch, W. *Eur. J. Inorg. Chem.* **2003**, *2003*(3), 506–513.
(32) Engelke, L.; Schäfer, M.; Schur, M.; Bensch, W. *Chem. Mater.* **2001**, *13*(4), 1383.
(33) Millange, F.; Medina, M. I.; Guillou, N.; Férey, G.; Golden, K. M.; Walton, R. I. *Angew. Chem., Int. Ed* . **2010**, *49*(4), 763–766.
(34) Walton, R. I.; O'Hare, D. *J. Phys. Chem. B.* **2001**, *105*(1), 91.
(35) Millange, F.; Serre, C.; Guillou, N.; Férey, G.; Walton, R. I. *Angew. Chem., Int. Ed.* **2008**, *47*(22), 4100.
(36) Kiebach, R.; Pienack, N.; Ordolff, M.-E.; Studt, F.; Bensch, W. *Chem. Mater.* **2006**, *18*(5), 1196–1205.
(37) Sharp, J. D.; Hancock, J. H. *J. Am. Ceram. Soc.* **1972**, *55*, 74.
(38) Finney, E. E.; Finke, R. G. *Chem. Mater.* **2009**, *21*(19), 4692–4705.
(39) Francis, R. J.; Price, S. J.; Evans, J. S. O.; O'Brien, S.; O'Hare, D.; Clark, S. M. *Chem. Mater.* **1996**, *8*(8), 2102–2108.
(40) Stock, N. *Microporous Mesoporous Mater.* **2010**, *129*(3), 287.

Table 1. Summary of Crystal Data, Intensity Measurement, and Structure Refinement Parameters for $Sm(O_3P\text{-}C_2H_4\text{-}SO_3)(H_2O)$ (**1**) and $Pr(O_3P\text{-}C_2H_4\text{-}SO_3)(H_2O)$ (**2**)

	compound **1**	compound **2**
formula	$C_4H_{10}O_7PSSm$	$C_4H_{10}O_7PSPr$
formula weight (g/mol)	383.52	374.05
crystal system	monoclinic	monoclinic
space group	$P2_1/c$ (No. 14)	$P2_1/c$ (No. 14)
a (pm)	1081.4(2)	1081.2(1)
b (pm)	1311.3(3)	1322.72(5)
c (pm)	710.58(14)	716.22(4)
β (deg)	104.51(3)	104.84(1)
V (10^6 pm^3)	975.5(4)	990.1(1)
Z	4	4
tot., uniq. data, R_{int}	8013, 1586, 0.050	7034, 1468, 0.063
observed data [$I > 2\sigma(I)$]	1303	1468
R1, wR2	0.0295, 0.0807	0.0285, 0.0837
GOF	0.98	1.16
Δe min./max. (e/Å^3)	−1.17, 0.79	0.808, −0,828

48 h at 150 °C. The solids were filtered off and washed with water. The products were characterized by XRPD, patterns are shown in Supporting Information, Figure S2, and the refined cell parameters are given in Supporting Information, Table S2.

Structure Determination. Suitable crystals of the compounds $Sm(O_3P\text{-}C_2H_4\text{-}SO_3)(H_2O)$ (**1**) and $Pr(O_3P\text{-}C_2H_4\text{-}SO_3)(H_2O)$ (**2**) were carefully selected from the HT experiments using a polarizing microscope. X-ray diffraction measurements were performed on a STOE IPDS diffractometer equipped with a fine-focus sealed tube (Mo K_α radiation, $\lambda = 71.073$ pm). For absorption correction the programs XRed and X-Shape were used.[41] The crystal structures were solved by direct methods with SHELXS-97 and refined using SHELXL-97.[42] For both compounds only non-merohedral twinned crystals were obtained. The reflections of both individuals were indexed separately using RECIPE, and integration of the intensities was performed using TWIN.[41] By this procedure overlapping reflections were omitted. Experimental data and results of the structure determination of compounds **1** and **2** are given in Table 1. Selected bond lengths are given in Supporting Information, Table S3. For both compounds, the hydrogen atoms of the water molecule could be localized from the difference Fourier map. The hydrogen bond lengths and angles are given in the Supporting Information, Table S4, and the H-bonding scheme is given in the Supporting Information, Figure S3.

In Situ Experiments. EDXRD experiments were carried out at HASYLAB, beamline F3 at DESY, Hamburg, Germany. The white synchrotron radiation (4 to 55 KeV) was detected by a liquid nitrogen cooled germanium semiconductor detector system. The detector angle was set to approximately 1.9°. The best results were obtained by collimating the beam to 0.2 × 0.2 mm^2. A microwave oven (Biotage Initiator) was modified to permit direct irradiation of the glass reactor (Supporting Information, Figure S6). One advantage of the microwave system is the online logging of the reaction conditions, that is, pressure, temperature, and stirring rates. For conventional heating a custom-made reactor system heated by an external thermostat (JULABO) was used.[31,32] The spectra were recorded with acquisition times between 30 and 120 s to get the best resolution at the given reaction temperature. For both heating methods exactly the same amounts of starting materials were used: 148 μL of 2 M H_3L, 1500 μL of water, 148 μL of 2 M $SmCl_3$, and 200 μL of 2 M NaOH solutions were mixed in a glass vessel and sealed. The reaction solutions were homogenized, and the first spectrum was taken directly after starting the heating. The reaction temperatures were set to 110, 120, 130, 140, and 150 °C.

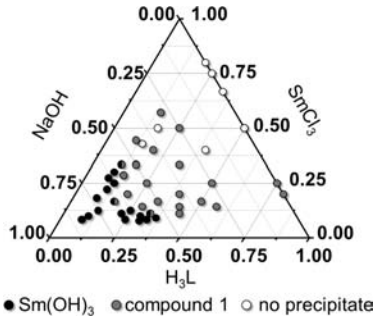

Figure 1. Crystallization diagram of the system $SmCl_3/H_2O_3P\text{-}C_4H_8\text{-}SO_3H$ (H_3L)/NaOH at 150 °C.

Results and Discussion

HT Study. The results of this investigation, based on the XRPD measurements are shown in Figure 1. In the ternary crystallization diagram only two compounds can be observed. At the molar ratios of $SmCl_3/H_3L$/NaOH 1−4:1−4:4−10 (pH > 10, Supporting Information, Table S1) only $Sm(OH)_3$ was obtained. At the molar ratios of 1−5:1−4:1−4 (pH 2−9, Supporting Information, Table S1) the title compound **1** was obtained. No precipitate was observed at very acidic conditions for the molar ratios of 1−4:1−2:0−3 at a (pH 1−2, Supporting Information, Table S1). At the molar ratio $SmCl_3/H_3L$/NaOH = 1:2:1 a non-merohedral twinned crystal was isolated.

Substituting Sm by La, Ce, Pr, Nd, Eu, or Gd leads to the formation of the isostructural compounds. The title compound **2** was isolated from these experiments, which also form twinned crystals. The powder patterns as well as the refined cell parameters of the isostructural compounds $Ln(O_3P\text{-}C_4H_8\text{-}SO_3)(H_2O)$ (Ln = La−Gd) are given in Supporting Information, Figure S2 and Table S2, respectively.

Crystal Structure of $Sm(O_3P\text{-}C_4H_8\text{-}SO_3)(H_2O)$. Since all title compounds are isostructural, the description of the crystal structure is given using the example of $Sm(O_3P\text{-}C_4H_8\text{-}SO_3)(H_2O)$ (**1**). It is not trivial to distinguish between phosphorus and sulfur employing X-ray scattering methods because of the similarity of the scattering factors. Both atoms have been differentiated by a comparison of the P−O and S−O bond lengths with bond length of lanthanide phosphonates and sulfonates as reported in the literature. For example the compounds $Sm[(O_3PCH_2)_2N(H)C_6H_4COOH]\cdot H_2O$,[43] $GdH[O_3P(CH_2)_3PO_3]$[44], and $La(O_3PC_6H_5)(HO_3PC_6H_5)$[45] show P−O bond lengths of 147(2)−155(1) pm whereas significantly shorter S−O bond lengths varying from 143(1) to 146(1) pm are observed for the compounds $La(CH_3SO_3)_3\cdot 2H_2O$[46] and $(C_{10}H_7SO_3)[Pr(C_{10}H_7SO_3)_2(H_2O)_6]\cdot H_2O$.[47] P−O bond lengths ranging from 149.0(1) to 155.2(4) pm and S−O bond lengths ranging from 145(1) and 147.3(4) pm were found for compounds **1** and **2** and agree very well with the literature data.

The three-dimensional structure is composed of Sm^{3+} and 4-phosphonatobutanesulfonate $(O_3P\text{-}C_4H_8\text{-}SO_3)^{3-}$ ions as well as one water molecule. The Sm^{3+} ions are

(41) *XRED version 1.19, X-Shape version 1.06, RECIPE, TWIN*; Stoe & Cie GmbH: Darmstadt, Germany, 1999.
(42) Sheldrick, G. M. *SHELXTL-PLUS Crystallographic System*; Siemens Analytical X-ray Instruments Inc.: Madison,WI, 1992.
(43) Bauer, S.; Bein, T.; Stock, N. *J. Solid State Chem.* **2005**, *179*, 145.
(44) Serpaggi, F.; Férey, G. *J. Mater Chem.* **1998**, *8*, 2749.
(45) Wang, R. C.; Zhang, Y.; Hu, H.; Frausto, R. R.; Clearfield, A. *Chem. Mater.* **1992**, *4*, 864.
(46) Wickleder, M. S. *Z. Anorg. Allg. Chem.* **2001**, *627*, 1675.
(47) Ohki, Y. S., Y.; Nakamura, M.; Shimoi, M.; Ouchi, A. *Bull. Chem. Soc. Jpn.* **1985**, *58*, 2968.

surrounded by eight oxygen atoms. Each rare earth ion is connected to six O_3P-C_4H_8-SO_3^{3-} ions through five P−O−Sm and two S−O−Sm bonds. The full coordination sphere is completed by the H_2O molecule (Figure 2). The oxygen atoms act as end on (O1, O5, O6) as well as bridging ligand atoms (O2, O3). Thus, edge-sharing of the SmO_8-polyhedra is observed that lead to the formation of chains along the *c*-axis. These chains are connected to layers by the phosphonate and sulfonate groups (Figure 3). The interconnection of the layers is accomplished through the -$(CH_2)_4$- group and a three-dimensional framework is formed. The structure is further stabilized by hydrogen bonds between the oxygen atom O4 of the sulfonate group and the coordinated water molecule (OW1) (Supporting Information, Figure S3, Table S4).

The obtained compounds are isoreticular to the previously reported series Ln(O_3P-C_2H_4-SO_3)(H_2O) with Ln = La, Ce, Pr, Nd, Sm, Eu, Gd, Tb, Dy.[12] The extension of the organic linker form -C_2H_4- with -C_4H_8- led to the extension of the spacing from 832.6 to 1046.9 pm between the inorganic layers.

IR and Raman Spectroscopy Study. Compound **1** was studied by IR and Raman spectroscopy (Supporting Information, Figure S4). The bands between 1250 and 950 cm^{-1} can be assigned to the P−C, P−O, S−C, and S−O stretching vibrations of the tetrahedral CPO_3- and CSO_3-groups. The broad band around 3421 cm^{-1} confirms the presence of water molecules that form H-bonds. The corresponding deformation band appears at 1662 cm^{-1}. Bands in the region from 3000 to 2900 cm^{-1} are due to CH_2 stretching vibrations. The corresponding CH_2-deformation vibration appears in the range of 1466 cm^{-1}.

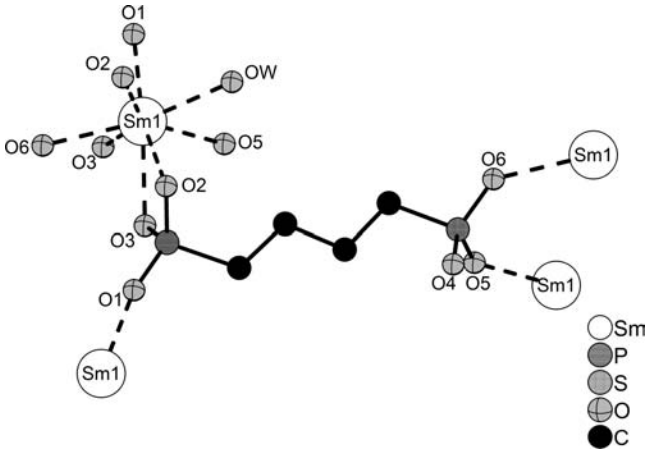

Figure 2. Coordination spheres of the Sm^{3+} ion in compound **1**.

Thermal Study. Thermogravimetric (TG) measurements were performed to gain deeper insight on the thermal stability of the title compound. The results of TG investigation (Supporting Information, Figure S5) show three steps of weight loss for Sm(O_3P-C_2H_4-SO_3)(H_2O). The loss of one water molecule per formula unit (observed, −5.1%; calculated, −4.7%) is found up to a temperature of 360 °C. The dehydrated sample can be heated up to 400 °C without any weight loss. Above this temperature the decomposition of the organic molecules takes place in two steps and leads to an X-ray amorphous residue. The dehydrated sample showed a poor crystallinity and could not be rehydrated with water.

In Situ X-ray Investigations. The formation of compound **1** was investigated by EDXRD measurement using conventional and microwave heating at 110−150 °C. The EDXRD spectra for the syntheses at 150 °C are shown in Figure 4.

Qualitatively both crystallization processes are independent of the heating methods. Therefore, the results obtained by conventional heating are described. During the first 5 min a modulation of the background in the range of 30−40 keV is observed (compare Supporting Information, Figure S7). This indicates the presence of an X-ray amorphous side phase in the first step of the reaction. Furthermore after 1 min a crystalline intermediate phase is detected. This phase transforms completely into compound **1** during the first 7 min. The transformation is apparent from the peak shift in the range 31−34 keV (Figure 5). In quenching experiments it was not possible to isolate the intermediate phase in reasonable crystallinity. Unfortunately the most intensive peak of the intermediate phase and the peak corresponding to the 100 reflection of compound **1** overlap strongly (33.20 keV (d = 1060 pm) vs 32.76 keV (d = 1027 pm)). Hence, for a quantitative evaluation, a data deconvolution was carried out by a brute force method assuming the overlapping peaks as a superposition of two Gaussians. For this time-consuming calculation the free parameters like the half-width, standard derivation, and the peak position had to be restricted to certain value ranges. For given boundaries, all possible superpositions of the two Gaussians were tested to get the best description of the obtained spectra. The transformation of the intermediate phase and the resulting normalized integrals

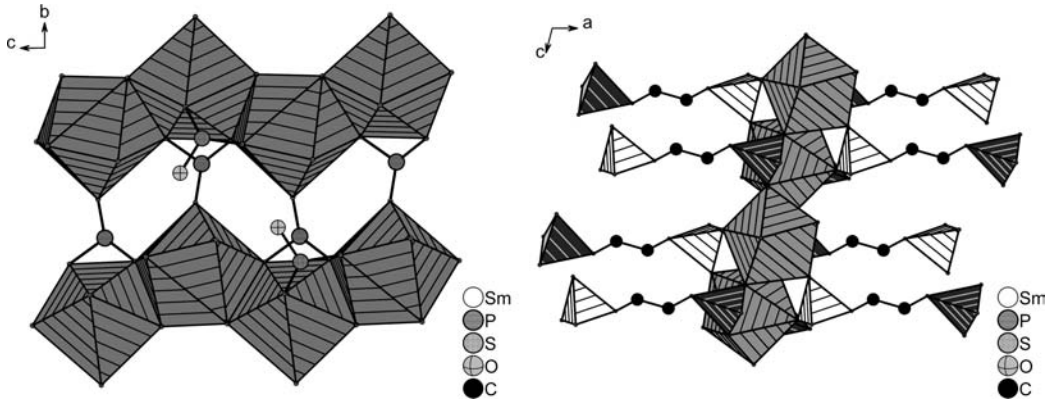

Figure 3. One-dimensional chains of edge-sharing SmO_8-polyhedra along the *c*-axis are connected by the sulfonate- and phosphonate groups. SmO_8-polyhedra are shaded in gray (left). The LaO_8-polyhedra-sulfonate/phosphonate layers are interconnected by the -$(CH_2)_4$- groups and form a three-dimensional network (right). The C-PO_3 tetrahedra are shaded dark gray and the C-SO_3 tetrahedra are shaded white.

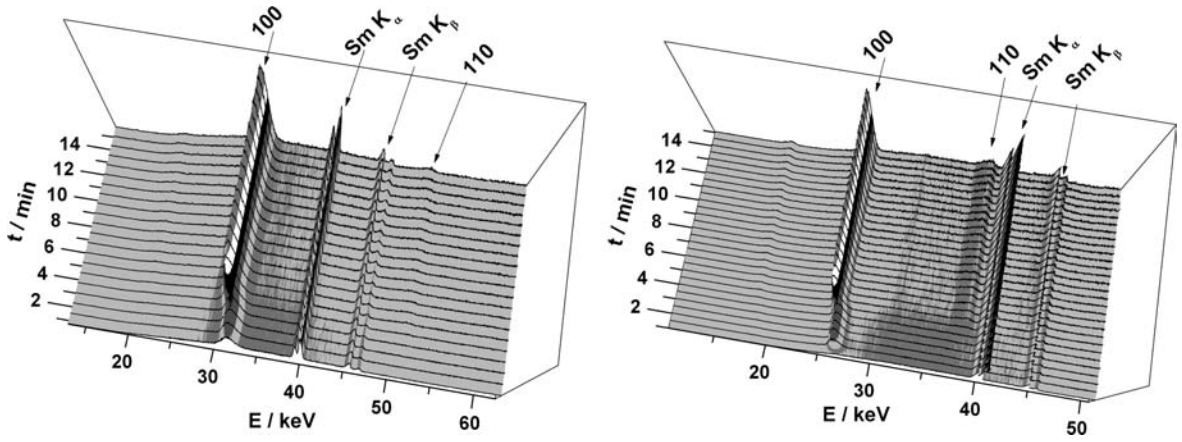

Figure 4. EDXRD patterns of the formation of compound **1** at 150 °C by conventional heating (left) and microwave heating (right).

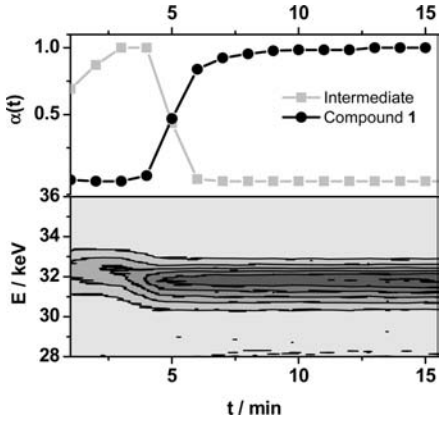

Figure 5. Surface plot of the transformation of the intermediate into compound **1** and reaction progress (α(*t*)) for both phases (conventional heating, 150 °C).

α(*t*) (reaction progress) are shown in Figure 5. After the transformation ($t > 6$ min) process, the intensity of the 100 peak of compound **1** is slightly increasing which indicates that the reaction is not finished.

For the kinetic analyses the reactions were repeated at different temperatures (110, 120, 130, and 140 °C). Microwave as well as conventional heating was employed to study the temperature dependence and influence of the heating method on the reaction (Figure 6). Differences in the heating progress are clearly visible for different temperatures. The curves show for both heating methods, that higher temperatures lead to faster reactions and shorter induction times as one might expect. The intermediate phase is observed in all reactions. For both heating methods similar induction times were found, ranging from 3 to 8 min. The differences substantiate a closer look at the rate of reaction, which turns out higher for the microwave heating. This is seen by comparing the reactions at 110, 120, and 130 °C. While almost no changes in reaction time are found in microwave heating, a significant increase in reaction time with decreasing temperature is observed when applying conventional heating ($t(\alpha = 0.5, T = 130\ °C) \sim 7$ min and $t(\alpha = 0.5, T = 110\ °C) \sim 18$ min, Figure 6 (top)).

A quantitative evaluation of the crystallization was established using the Sharp−Hancock analysis[37] The Sharp−Hancock equation $\ln[-\ln(1 - \alpha)] = m \cdot \ln(k) + m \cdot \ln(t_{red})$ yields by linear regression the reaction exponent m (Avrami exponent) and the rate constant k from the intercept $m \cdot \ln(k)$; α denotes the degree of crystallinity and t_{red} the aging time. All Sharp Hancock plots are given in the Supporting Information. The obtained reaction exponents and rate constants are summarized in Table 2 and 3.

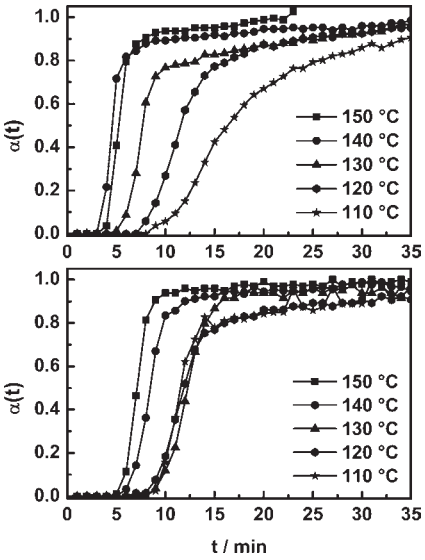

Figure 6. Normalized intensities of the 100 peak from the EDXRD measurements taken at different temperatures using conventional (top) and microwave heating (bottom). For clarity, the formation of the intermediate is not shown.

Table 2. Reaction Exponents m and Rate Constants Obtained from the Sharp−Hancock Analyses for the Early Reaction Step

T [°C]	m microwave	k [s^{-1}] microwave	m conventional	k [s^{-1}] conventional
110	2.9(1)	4.40×10^{-3}(4)	2.3(1)	2.49×10^{-3}(1)
120	2.0(2)	5.44×10^{-3}(4)	2.21(4)	3.34×10^{-3}(5)
130	2.80(1)	5.5×10^{-3}(1)	3.1(1)	5.40×10^{-3}(4)
140	2.2(2)	8.33×10^{-3}(5)	2.1(1)	4.70×10^{-3}(6)
150	2.11(7)	1.26×10^{-2}(4)	3.0(1)	9.9×10^{-3}(1)

Compound **1** is formed in two steps. In the early reaction stage, the transformation of the intermediate phase into compound **1** takes place. Here, reaction exponents varying from $m \sim 2.1$ to $m \sim 3.0$ were determined for both heating methods indicating a nucleation controlled reaction mechanism.[37] After the complete transformation into compound **1**, the reaction is still not finished, and the 100 peak increases

Table 3. Reaction Exponents m and Rate Constants Obtained from the Sharp−Hancock Analyses for the Late Reaction Step

T [°C]	m microwave	k [s^{-1}] microwave	m conventional	k [s^{-1}] conventional
110	0.68(1)	1.97×10^{-3}(1)	0.29(1)	1.74×10^{-2}(5)
120	0.60(2)	4.74×10^{-3}(4)	0.3(1)	2.25×10^{-2}(4)
130	0.34(3)	1.08×10^{-3}(5)	0.3(1)	4.65×10^{-2}(3)
140	0.3(2)	9.05×10^{-2}(4)	0.31(4)	7.41×10^{-2}(5)
150	0.37(3)	5.02×10^{-2}(6)	0.23(7)	9.6×10^{-2}(1)

further. For the late reaction step, Avrami exponents between $m \sim 0.23$ and $m \sim 0.68$ were obtained which suggest a diffusion controlled mechanism. The model with the lowest Avrami exponent is a diffusion controlled reaction mechanism having a value of 0.62.[37] Smaller values have been reported previously and explained by hindered diffusion.[48,49] It should be noted that the reaction mechanism models are empirical and have widely been applied to many reaction systems, even to crystallizations from sol−gels.[38] Furthermore, the models have previously been used for reactions where crystalline solids are formed directly from the reaction mixture, that is, without the formation of an intermediate. Nevertheless, this method allows to extract the rate constants and enables the comparison of reactions, for example, at different temperatures.

The obtained rate constants at different temperatures allow the determination of the Arrhenius activation energy and the pre-exponential factor for both heating methods (see Supporting Information). For the first reaction step an activation energy for the phase transition from the intermediate phase into compound **1** was determined as 34(7) kJ/mol with an pre-exponential factor of 3(1) for the microwave reaction and 41(9) kJ/mol with an pre-exponential factor of 4(1) for the conventional reaction. Within the precision of the measurement the values are independent of the heating methods. In the literature no values for the activation energy for the formation of phosphonates are given yet. A comparison with inorganic solids that form under nucleation controlled reaction mechanisms shows only slightly higher values. Thus, for the formation of zeolite A, barium titanate, or Mg−Al hydroxide an activation energy of 58, 55, and 41 kJ/mol was determined, respectively.[50−52] For the second reaction step the observed activation energies differ significantly. For microwave and conventional heating activation energies of 62(6) kJ/mol and 128(27) kJ/mol were calculated. The pre-exponential factors were determined as 33(8) and 15(2) for microwave and conventional heating, respectively. This phenomenon has been previously observed. For the heating induced decomposition of sodium bicarbonate to sodium carbonate significant reduction of the activation energy was determined for the microwave heating method.[53] In another study on synthesis of titanium carbide the increase of the pre-exponential factor was observed for the microwave reactions. It was concluded that the mobility of molecules can be increased in presence of a microwave field.[54]

Conclusion

HT methods help to discover new compounds and to establish their fields of formation. While normally reaction times in the range of days are used, the in situ study shows that in our case metal phosphonatosulfonates are formed in the range of minutes, and an intermediate phase is observed. From the in situ experiment it can be concluded that within the temperature range 110−150 °C the reaction proceeds in two steps for microwave as well as for conventional heating. While no influence on the phase transition between the intermediate and compound **1** is observed, differences are found for the ongoing crystallization after the transformation. At the late reaction step, conventional heating leads to significantly higher activation energies and lower pre-exponential factors than the microwave heating which could be due to a higher mobility of the ions under microwave irradiation. The study presented here shows that a combination of HT methods and in situ EDXRD measurement supports the efficient investigation of solvothermal reaction systems regarding the determination of fields of formation and the evaluation of crystallization processes.

Acknowledgment. We thank the HASYLAB, Hamburg for the beamtime and the DFG (project STO 643/2) for the financial support.

Supporting Information Available: Supporting Information with exact amounts used for the HT synthesis, XRPD patterns, selected bond distances, H-bonding figures, and results of the EDXRD study are available. This material is available free of charge via the Internet at http://pubs.acs.org. The Cambridge Crystallographic Data Center (CCDC) 790588−790589 contains the supplementary crystallographic data for this paper. These data can be obtained free of charge via the Internet at ww.ccdc.cam.ac.uk/conts/retrieving.html (or from the CCDC, 12 Union Road, Cambridge CB2 1EZ, U.K; fax, +44 1223 36033; e-mail, deposit@ccdc.ac.uk).

(48) Pradell, T.; Crespo, D.; Clavaguera, N.; Clavaguera-Mora, M. *J. Phys. Cond. Matter*. **1998**, *10*, 3833.
(49) Kozlovsky, M. V. *Cryst. Res. Technol*. **2001**, No. 36, 1083.
(50) Davies, A. T.; Sankar, G.; Catlow, C. R. A.; Clark, S. M. *Phys. Chem. B* **1997**, *101*, 10115.
(51) Millange, F.; Walton, R. I.; O'Hare, D. *J. Mater. Chem*. **2000**, *10*, 1713.
(52) Walton, R. I.; Millange, F.; Smith, R. I.; Hansen, T. C.; O'Hare, D. *J. Am. Chem. Soc*. **2001**, *123*, 12547.
(53) Shibata, C.; Kashima, T.; Ohuchi, K. *J. Appl. Phys*. **1996**, *35*, 316.
(54) Binner, J. G. P.; Hassine, N. A.; Cross, T. E. *J. Mater. Sci*. **1995**, *30*, 5389.